The time-derivative of the kilohertz quasi-periodic oscillations in the neutron star 4U 1702–429

Mathijs van de Mast

December 6, 2012

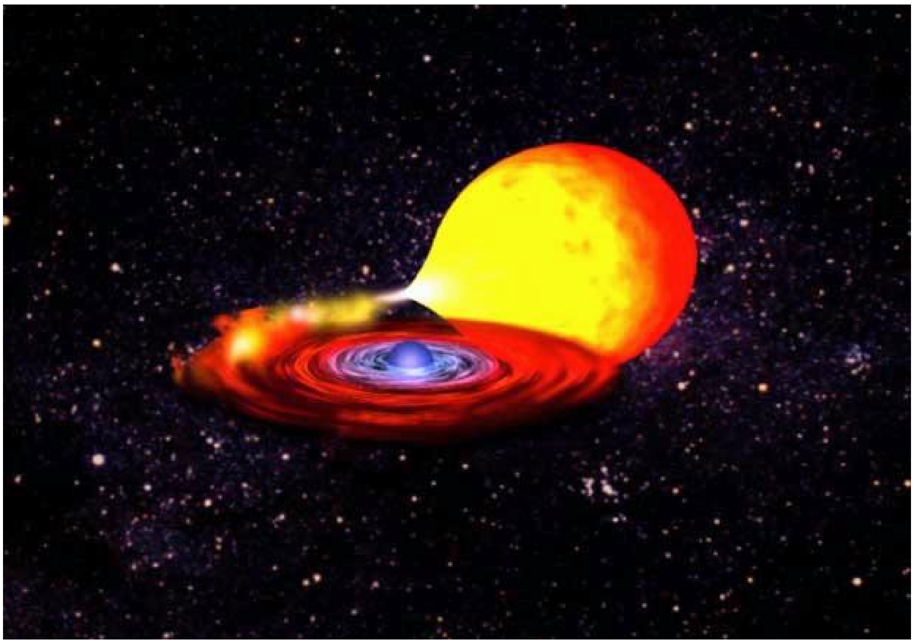

Artist's rendition of a neutron star accreting matter from a companion star. Image: NASA.

Supervisor: Prof. Dr. Mariano Méndez
Kapteyn Astronomical Institute
Rijksuniversiteit Groningen

Contents

Abstract

I investigated the time variability in the spectra of the neutron star low-mass X-ray binary 4U 1702–429, observed with the Rossi X-ray Timing Explorer. In 27 of the 226 observations the power spectra showed a Quasi Periodic Oscillation (QPO) ranging from 600 to 940 Hz. In six of these observations I found another QPO alongside the previous one, ranging from 975 to 1080 Hz. From these six observations a linear relation between upper and lower QPO frequencies was found to be: $\nu_{upper} = 1.04\nu_{lower} + 304.3$ Hz. I calculated the time-derivatives of the QPO frequencies ($\dot{\nu}_{QPO}$) across every time interval between two successive power spectra. The 3176 accepted time intervals ranged from 32 s to 176 s, with a median of 48 s. Plotting the $\dot{\nu}_{QPO}$ values against the centroid frequency of the QPO, I found (i) a considerable similarity between the magnitude of positive and negative $\dot{\nu}_{QPO}$ values, and (ii) that $\dot{\nu}_{QPO}$ values calculated over long and short time intervals lie together closely at each centroid frequency. I concluded that there is in all likelihood a coupling between the mechanisms that increase and decrease the QPO frequency. The absolute values ($|\dot{\nu}_{QPO}|$) of all data together show a more or less constant $|\dot{\nu}_{QPO}|$ range of 0 to 0.065 Hz s^{-1} over the entire range of centroid frequencies. This is not at variance with the findings of Sanna et al. (2012), who found an anticorrelation between $|\dot{\nu}_{QPO}|$ and centroid frequency of QPOs in the neutron star 4U 1636–53, within this range. The spread in my $|\dot{\nu}_{QPO}|$ values, though, is too large to actually verify this anticorrelation. Following the study by Sanna et al. (2012), I tested whether the measured $|\dot{\nu}_{lowerQPO}|$ and the calculated $|\dot{\nu}_{upperQPO}|$ data could be reproduced by the standard disc theory by Shakura and Sunyaev (1973) under the assumption that the QPO frequency corresponds to the Keplerian orbit at the sonic-point radius, taking into account the effects of radiation drag. For both upper and lower frequency QPOs I found a simulation of a rather heavy neutron star to reasonably reflect the measured and calculated $|\dot{\nu}_{QPO}|$ - centroid frequency behaviour. Given the errors in my $|\dot{\nu}_{QPO}|$ values, though, this agreement is not very conclusive.

1 Introduction

In a nutshell, the problem of the Kilohertz Quasi Periodic Oscillations (KHz QPOs) is the following: When looking at the time variability in the X-ray emission of a neutron star's accretion disk, (id est: taking the power spectrum of a continuous observation), one may find one or two special features. Mathematically speaking, some time variability called broadband noise on scales of 10^{-5} to a few hundred Hz is very common (Hasinger & van der Klis et al. 1989). The power spectrum decreases to a noise level of order 2 around a frequency of a few hundred Hz. At frequencies of 300 – 1200 Hz, though, some power spectra show one or two peaks, which are until today ill-understood and ill-explained (Strohmayer, Zhang & Swank, 1996; van der Klis, 2005). Usually, the peak at the lower frequency occurs between 500 and 950 Hz, and is a good deal stronger and narrower than the one at higher frequency peak (see section 2.2). With a full width at half maximum of order 5 – 100 Hz, these peaks are called quasi-periodic oscillations (Markwardt et al. 1999). The frequencies at which these KHz QPOs (hereafter: QPOs) occur can change by tens of Hz over the course of a few hundred seconds (Berger et al. 1996). See figure 1.
This phenomenon has been studied for 15 years now, and several different models have been

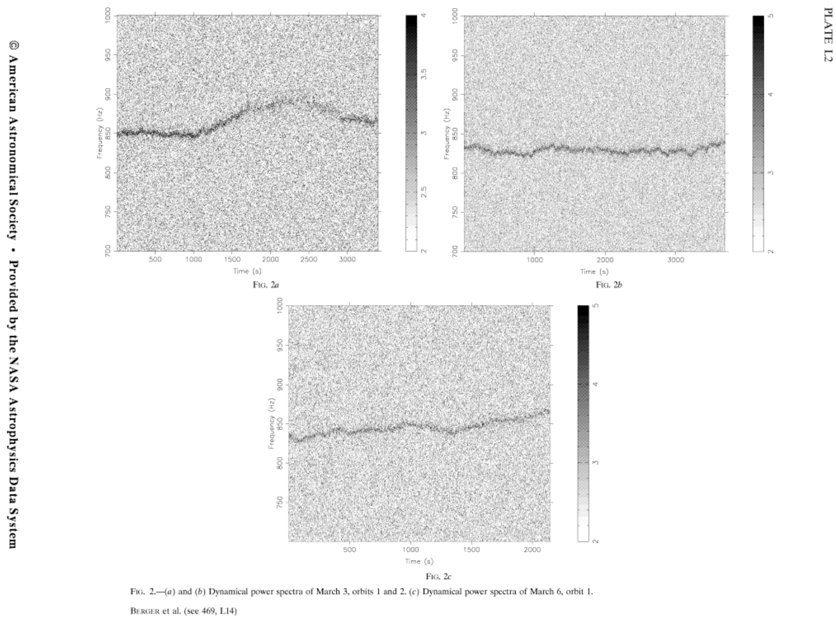

Figure 1: *Time evolution of the QPO frequency in the neutron star 4U 1608–52. Image: Berger et al. (1996).*

proposed to explain these QPOs (e.g. Miller, Lamb & Psaltis, 1998; Stella & Vetri, 1998), but none of them is yet widely accepted. Sanna et al. (2012) studied the neutron star 4U 1636–53, and for the first time measured the rate at which the QPO frequency changes over time. They found that the negative and positive time-derivatives of the QPO frequencies (hereafter: $\dot{\nu}_{QPO}$) at any given time had a close agreement in magnitude, which suggests a coupling in the mechanisms for increasing and decreasing the QPO frequency. They also found an anticorrelation between the centroid frequency of the QPO and the magnitude of the time-derivative of that frequency ($|\dot{\nu}_{QPO}|$). Finally, they also found that the average $|\dot{\nu}_{QPO}|$ decreased by a factor of

2 as the time intervals over which those $|\dot{\nu}_{QPO}|$ values are calculated increased from less than 64 to 160 s.

Following in the footsteps of the study by Sanna et al. (2012), I have tested the neutron star 4U 1702−429 (hereafter: 4U 1702) for these same findings. An agreement between these two neutron stars could point to the validity of any physical model that reproduces these measurements.

The Rossi X-ray Timing Explorer (RXTE) collects information on the time variations of X-ray sources. It orbits around Earth every 90 minutes, and it has three different instruments on board. The observations relevant for my study of neutron star 4U 1702 were made with the Proportional Counter Array (PCA). This instrument consists of five Proportional Counter Units (PCUs). Each PCU consists of five layers, the middle three of which are split in two. The depth of the layer in which a particle (be it a photon or a cosmic ray) is detected is one rough measure of its energy. The PCUs map the energies of incoming particles into different channels as a more detailed energy measurement, with an accuracy of 1 μs. The PCUs then send detailed information of their measurements to six units in the Experiment Data System (EDS), which pack information of the measurements in specific ways. Four of the EDS units can be tuned to the desired temporal and energy resolutions, and information on the PCU number, layer and half in which photons are detected can be packed in user-defined ways. To facilitate comparison of observations with different resolutions, one EDS unit named Std.1 is always kept at a time resolution of 1/8 s and the energy resolution of one energy channel. The last, named Std.2 is always kept at a time resolution of 16 s and an energy resolution of 129 channels between 2 and 60 keV. Observations of the neutron star 4U 1702 were taken over the course of a number of years. The observation data consist of X-ray photon counts, which show the intensities at different energies of X-ray radiation from the source as a function of time. These light curves show variability of intensity on different time scales, the shortest of which, we are interested in.

Binary star systems with one star and one compact X-ray emitting object are generally characterised by the mass of the companion star. If the mass of the companion star exceeds that of the compact object, it is called a high mass X-ray binary (HMXB). If the companion star is below that threshold, we speak of a low mass X-ray binary (LMXB). The neutron star 4U 1702 is located in an LMXB.

In the companion star, matter flows around in a potential field defined by the distribution of mass in the neutron star and the star itself. Close to the centre of mass of the star, this potential field is spherically symmetric, and hence the star is spherical. Closer to the neutron star, though, the neutron star pulls the potential field towards the centre of mass of the system. In this type of potential field, the boundary of the region in which matter is still gravitationally bound to the star is marked by a Roche lobe. If there is matter in the star that exceeds the extent of the star's Roche lobe, this matter can be attracted to the neutron star. See figure 2. Due to the fact that both bodies are orbiting around a common centre of mass, there is a rotational pseudoforce to be considered, and from the system's rest frame, matter does not fall to the neutron star straightly. Rather, it spirals in closer to the neutron star, forming an accretion disc.

Geometrically, this is a very thin disc, lying in the plane of the neutron star's motion around the centre of mass. Because of the annular shape, matter in this disc does not move in Keplerian orbits. Any particle is subjected to not only the gravitational forces causing it to revolve around the neutron star, but also to friction with particles at larger and smaller radii, which move slower and faster, respectively. From the particle's rest frame, the material farther out at higher-radius orbits is moving backwards, and material closer to the neutron star is moving forward. The friction with these neighbouring particles causes the particle to lose angular momentum, and thus fall closer to the neutron star gradually, ultimately reaching the neutron star surface, and becoming part of it.

According to Shakura and Sunyaev (1973) matter in a geometrically thin disc moves radially

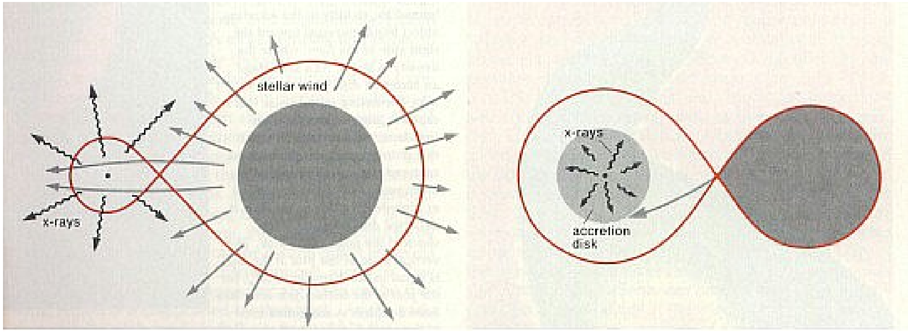

Figure 2: *The red lines indicate the equipotential surfaces beyond which matter is no longer gravitationally bound to the massive bodies at their centres. The left panel shows an HMXB, the right shows an LMXB. Image: Figure 3 from The Hydrodynamics of Accretion from Stellar Winds, Ronald E. Taam & Bruce A. Fryxell, American Scientist, November-December 1989, pp. 539-545.*

with a speed given by:

$$v_r = 0.98\alpha_s^{4/5}\dot{M}^{3/10}M_\star^{-1/4}R^{-1/4}f^{-14/5}\text{km s}^{-1} \tag{1}$$

with

$$f = \left[1 - \left(\tfrac{R_\star}{R}\right)^{1/2}\right]^{1/4}$$

and $\alpha = 0.1\alpha_s$ is the viscosity parameter, $\dot{M}$ is the mass accretion rate in units of 2.6×10^{17} g s^{-1}, $M_\star = M/1.8M_\odot$, R is the radius of the inner edge of the disc in km and $R_\star$ is the neutron star radius in units of 14 km, respectively. (Sanna et al. 2012).

In some occasions, this accretion disc does not reach down continually to the neutron star surface, but it is truncated at some inner radius. Below are mentioned two specific mechanisms which could independently explain this disc truncation: the Sonic Radius (Miller et al. 1998) and the Inner Stable Circular Orbit (Barret et al. 2005).

The velocity of a particle in the accretion disc can be expressed in two components: the radial and orbital. The presence of the radial component (pointing inward towards the neutron star) constitutes the deviation from Keplerian orbit. This radial component is relatively small at large radii, but gets larger when the particle spirals closer to the middle. At some radius, this radial velocity exceeds the sonic velocity, the speed of a hydrodynamic signal in that particular medium. This radius is called the Sonic-Point radius, and from here the particle falls towards the neutron star so rapidly that there is no spiralling accretion disc any longer.

The Inner Stable Circular Orbit (ISCO) is determined by general relativity. The theory of general relativity states that the gravitational potential resulting from a massive body as a function of the distance to that body does not diverge to infinity at $r \to 0$, but rather rather makes a sharp bend downwards at a very small radius, and diverges to minus infinity from there. At radii above the one at which this bend occurs, stable orbits are possible (elliptic, circular, parabolic or hyperbolic, be it with some precession, depending on the energy of the particle). At radii below this threshold, stable orbits do not occur, matter flows to the middle rapidly, and no accretion disc can exist.

2 Observation and data analysis

I was provided with 226 observations from the RXTE archive, which Andrea Sanna had downloaded. Each observation shows a power spectrum of the source at a given time. The observations all have zero, one or two QPOs. I looked at all the power spectra to determine whether they show zero, one or two QPO-like peaks. I found 24 observations with a QPO, which I called “good”, and I found 135 with no QPO, and 67 of which I was not certain, these I called “doubtful”.

2.1 Fourier transformation of the RXTE observations

The observations of the X-ray signals from 4U 1702 were transformed to power spectra. The intensity of the signal at a specific time is a real valued quantity. When the time signal is multiplied by a complex e-power of frequency and integrated over time, a complex number is obtained for every frequency. The power spectrum is a plot of the absolute value ($\sqrt{\Im^2(a)+\Re^2(a)}$) of the transformed number at every frequency. It is a truth inherent to the mathematics of the Fourier transform that the magnitude of the noise on this power spectrum is equal to the power itself (e.g. Bendat & Piersol, ’Random Data, Analysis and Measurement Procedures’, 2010). This noise can be reduced by breaking up the observation into pieces. Every observation from the PCA has been broken in pieces of 16 seconds. Each of these pieces is separately transformed into a power spectrum called a “trafo”. This means that the lowest frequency that can appear on the power spectrum is 1/16 Hz. (No wave with a period longer than 16 seconds can be found on a section of observation that is only 16 seconds in length). The time resolution of the RTXE measurements also sets an upper limit to the frequencies that can appear on the power spectra, this is the Nyquist frequency, which is $\nu_{Ny} = \frac{1}{2\Delta t}$, where Δt is the time resolution of the light curve. No wave with a period shorter than twice the time resolution of an observation can be seen. The time resolution of the PCA observations is at least 1/4096 s, this makes the Nyquist frequency 2048 Hz.

The power spectra of different trafos are combined into one power spectrum. Taking a long trafo length increases the frequency range which can be transformed to, but taking a larger number of shorter trafos reduces the noise by a factor equal to the square root of the number of trafos which are taken.

A program called *fft_xte* (short for “fast fourier transform _ X-ray timing explorer”) takes photon counts from an observation and transforms it into a three-dimensional body of data. This data consists of a Fourier power for every observed frequency with a resolution of 1/16 Hz, on every observed point in time, with a resolution of 16 s. An observation can be analysed with a program called *dynspec*. *Dynspec* allows for viewing of selections of an observation. A QPO can be recognised if the frequency-time plane contains a significant peak of Fourier power at roughly the same frequency throughout an appreciable span of time. *Dynspec* allows for these planes to be plotted with different rebinning in frequency and time, so that a sequence of peaks in the Fourier power may be better visible. See figure 3.

I wrote a shell script, *tramaker*, that makes transformations of a large number of observations in one go. My script automatically operates the *fft_xte* software to bin all observations in time by a factor 2. I used this script on all good and doubtful spectra, so that by inspection of the trafos I could make a further selection of a few useful observations. With the help of my program *scriptwriter* I also wrote a script called *dynner* that uses *dynspec* on a large number of trafos, views them (minimum power: 1.7; maximum power: 2.3; minimum frequency: 400 Hz; maximum frequency: 1600 Hz) in four different time rebin factors (5; 10; 15 and 20), and four different frequency rebin factors (16; 64; 128 and 256), and exports one image for every

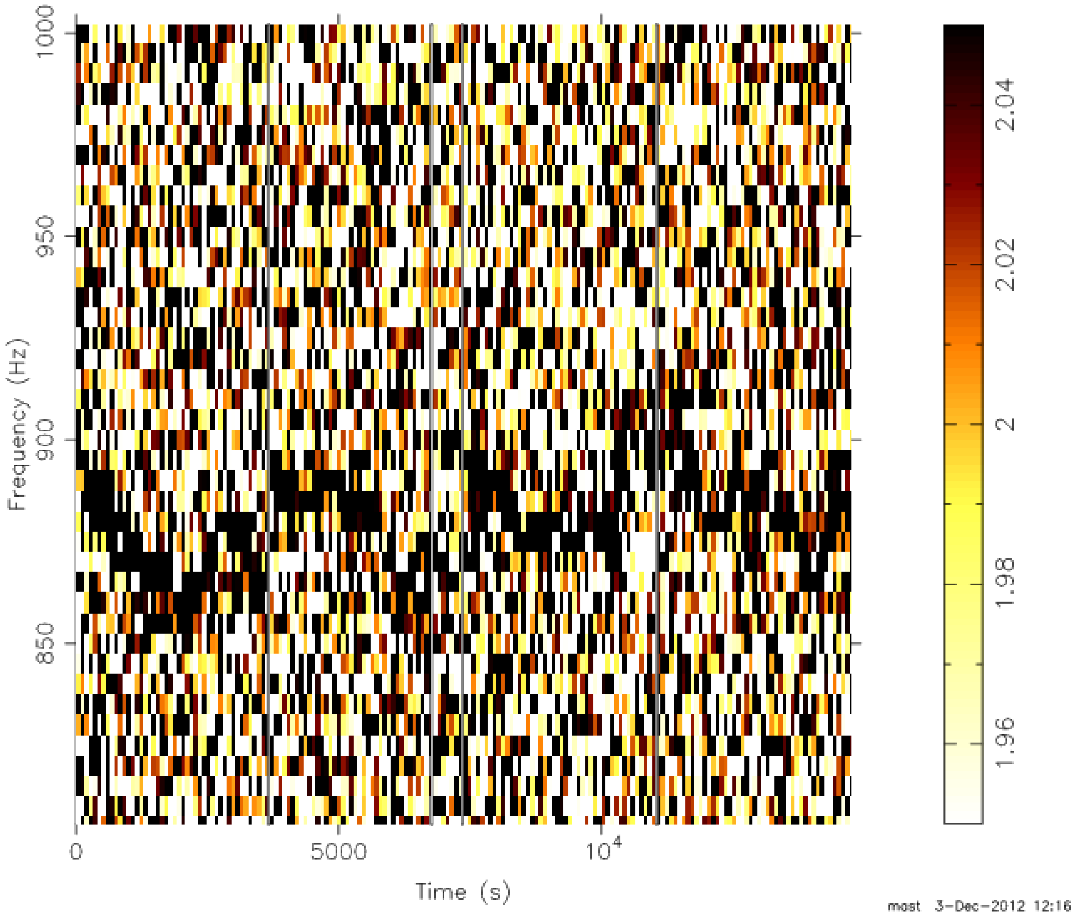

Figure 3: Dynspec *image of observation 80033-01-05-00 of X-ray source 4U 1702–429. At every point in the frequency-time plane, the Fourier power is given by the shade. It runs between 1.95 (light) and 2.05 (dark). The time rebin factor is 5, and the frequency rebin factor is 80. The movement of the peak frequency in time is visible as a dark line in this plane. The vertical lines show points in time at which no observations were made for a prolonged time (for instance due to instrument inactivity).*

combination of these rebins (i.e. 16 images for every observation). This script uses 16 rc files for every observation, I wrote a python script called *dynrcwriter* to generate these rc files.

The result was 1456 postscript images, containing different "faces" of the observations I had initially marked either good or doubtful. Viewing these images would help in a second assessment of whether the observation shows a good QPO. I found that the observations with two alleged QPOs only show at most one QPO significantly in *dynspec*. I developed a way to view all these images in succession, with notice of which observation, which time rebin and which frequency rebin is shown. Scrutinising different faces of doubtful and good trafos, I selected 6 observations which had a QPO I was previously unaware of, and unmasked three observations which unexpectedly had no significant QPO.

2.2 QPO identification

Lower QPOs are nearly always considerably more significant than the upper QPOs[1]. Therefore, we are very confident that all the QPOs we have found are lower QPOs. There are, however, two methods to increase that confidence.

An X-ray spectrum can be characterised by its hard and soft colours. In our case, hard colour is defined as the ratio between photon counts with energies $\in [9.7KeV; 16.0KeV]$ and photon counts with energies $\in [6.0KeV; 9.7KeV]$. Soft colour is defined as the ratio between photon counts with energies $\in [3.5KeV; 6.0KeV]$ and photon counts with energies $\in [2.0KeV; 3.5KeV]$. Guobao Zhang wrote a program based on *NASA HEAsoft* that accepts the sprectra of a number of observations, and calculates the corresponding soft and hard colours. This program takes into account the fact that the energies corresponding to different PCA channels change as the instrument gets older, the fact that different PCUs may collect photons from different fields of view, and that different PCUs may map energies onto channel numbers in different ways depending on how they are tuned. It normalises colours and intensities to those of the Crab Nebula.

When, of a number of X-ray binary spectra, the hard colours are plotted against the soft colours, the points usually form a banana shape on the diagram (Di Salvo et al. 2001). Points corresponding to spectra with a lower QPO in them usually have a low soft colour and a low-to-intermediate hard colour, thus lying somewhere near the middle of the banana. This is for no a priori known reason (Altamirano, et al. 2006). Guobao Zhang entered the spectra of all the 226 RXTE observations of neutron star 4U 1702 in his program, and the resulting soft colour-hard colour plot indeed shows a banana shape. He also entered the spectra of only the 27 ostensibly lower QPO observations, and the resulting soft and hard colours, when plotted over the earlier diagram, all lie near the middle of the banana. See figure 4.

Another method of separating lower and upper QPOs is by plotting the centroid frequencies of the QPOs versus the hard colours of the spectra. On such a plot, upper and lower QPO spectra fall in two distinct branches. Also this is for no a priori known reason, but separate branching of upper and lower QPOs on the frequency - hard colour plane has been reported for neutron star 4U 1636–53 (Belloni et al. 2007; Sanna et al. 2012), for neutron star 4U 1728–34 (Méndez et al. 1999) and for neutron star 4U 1608–52 (Méndez and van der Klis 1999).

With a piece of software called *xana*, I aligned all power spectra from different time indices in the same observation in such a way that the QPOs all share the same frequency, and then averaged those power spectra together. For most of the 27 observations, the resulting spectrum shows a sharp peak for the lower QPO, and for some observations, a less significant peak is observed some ~ 340 Hz higher, evidence of either an upper QPO or an unluckily positioned lump of noise. Six of the observations I analysed had two peaks, to which I fitted two Lorentzians plus a constant of order 2, and determined the presence of an upper QPO by two statistical arguments: 1) A measure of the significance of a peak is given by the ratio between the integral power of the fitted Lorentzian and its error. In my case, this ratio ranged from 2.83 to 3.62. Usually, a threshold of 3 is set to identify a QPO with sufficient confidence, but 2) the upper QPOs are all found at roughly the same frequency separation (340 ± 14.0 Hz) from their lower twin. A roughly fixed frequency separation between two twin QPOs from the same observation has been found for several QPOs (Sanna et al. 2012 found a separation close to 300 Hz for neutron star 4U 1636–53). The probability of a peak of noise appearing with such a significance and so close to the frequency where an upper QPO would really be expected is low enough so that we can confidently speak of six upper QPOs.

Figure 5 shows the frequencies and hard colours of my upper and lower QPO spectra, over-

[1]M. Méndez, priv. comm.

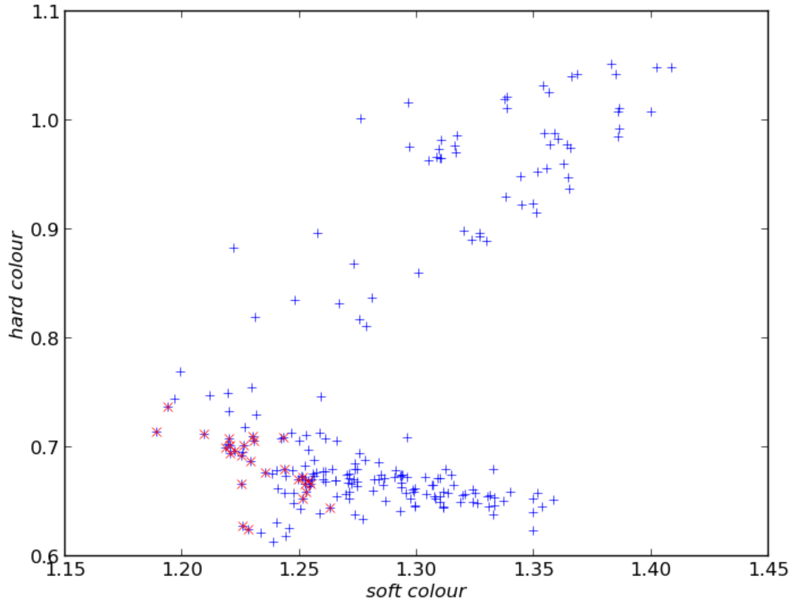

Figure 4: *Hard colour vs. Soft colour plot of all RXTE observations of neutron star 4U 1702-429. Blue plusses show all observations, forming the usual banana shape. Red X'es show observations with an assumed lower QPO.*

plotted with the upper and lower QPO data that Andrea Sanna calculated from the neutron star 4U 1636–53.

It is noticeable that the same types of QPOs from the two different neutron stars do not overlap on this plot. Both Andrea Sanna's data analysis and mine wield exactly the same definitions of soft and hard colours, and both have colours and intensities normalised to those of the Crab nebula. However, the apparent colours of a source can be influenced by interstellar absorption (which is more efficient in the low-energy regions). Internally, it can vary with the ratio between emission from the the neutron star surface (which dominates the middle part of the X-ray spectrum) and the corona component (which dominates the high-energy end of the spectrum). Also, the frequency separations between the upper and lower QPOs is not the same for both sources. See section 3.

2.3 Time-evolution of the lower QPO frequencies

With confidence of having 27 lower QPO observations, each with a power spectrum for a number of different time indices, the time evolution of the QPO frequency can be analysed. *Dynspec* lets a user trace the time evolution of a QPO frequency by selecting a sequence of points in the frequency-time plane. It can search for frequencies with the maximum count rate in the vicinity of the selected frequency at each point in time, or fit Lorentzians plus constants to the count rates in the vicinity of the selected frequency. The time-evolution of a QPO frequency can be exported into a file. For this it is important to find the lowest rebinning factors for frequency and time at which the QPO is still visible. At higher rebinning factors, the QPO is easier to see, but temporal- and frequency resolution is lost.

I used *dynspec* on all 27 observations, searched for the minimum frequency and time re-

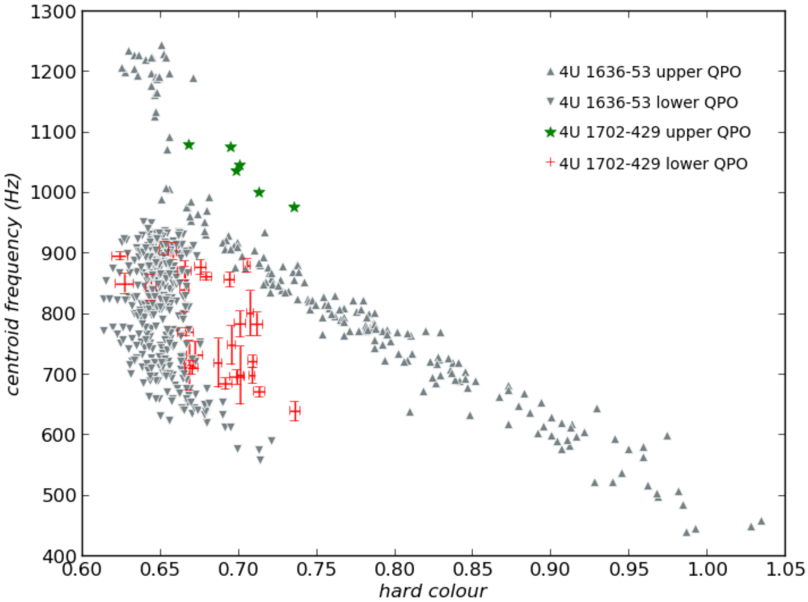

Figure 5: *Centroid frequency vs. hard colour of all QPO observations from neutron stars 4U 1636–53 and 4U 1702–429. Grey upward and downward triangles show the upper and lower QPOs, respectively, which have been found by Andrea Sanna in 2012. Green stars show my upper QPOs, and red error bars show my lower QPOs.*

bin factors, and traced the QPO frequencies for every point in time. The tracing methods of finding maxima and of fitting elevated Lorentzians to every single frequency profile (or a few permutations of those) result in frequency-time diagrams with lots of heavy fluctuations, even if the considered frequency range is limited to only 10 or 20 Hertz. When setting frequency limits for fitting a Lorentzian to the power spectrum, the peak of that Lorentzian is permitted to lie outside of that range, as long as the fit within the specified range adheres to the data. Calculating $\dot{\nu}_{QPO}$ from these traces yielded a lot of data with too high positive or negative derivatives. I used the linear interpolation between the points I selected in dynspec to calculate time-derivatives from. Figure 6 shows the time evolution of the QPO frequency as traced by the manual selection of points (thick black line), fitted elevated Lorentzians within 50 Hz from the selected points (green line), taken as the maximum within 20 Hz from Lorentzian fits (red line), and taken as maximum within 20 Hz from selected points (blue line) from observation 80033-01-02-00.

As can be seen in figure 6, there are some time intervals in the frequency evolution diagrams in which no measurements are taken, this was due to inactivity of the instrument (usually because the source was not visible form the RXTE's position in orbit). When calculating $\dot{\nu}_{QPO}$ values from this frequency evolution data, these gaps must, of course, be omitted, the slopes through those gaps are not implied by actual movement of the QPO frequency. I wrote a script called *gapfilter*, that parses all the time intervals of successive points in the frequency evolution data of all 27 observations. It stores in a separate file the temporal indices just prior to every gap which is longer than a certain threshold. I found that a threshold of twice the minimum time interval of each observation is a suitable choice: every accepted interval fell far beneath it, and every unacceptably long gap fell far above it. Most observations had no gaps to be omitted, as figure 6 suggests, observation 80033-01-05-00 had 3, one observation even had as many as

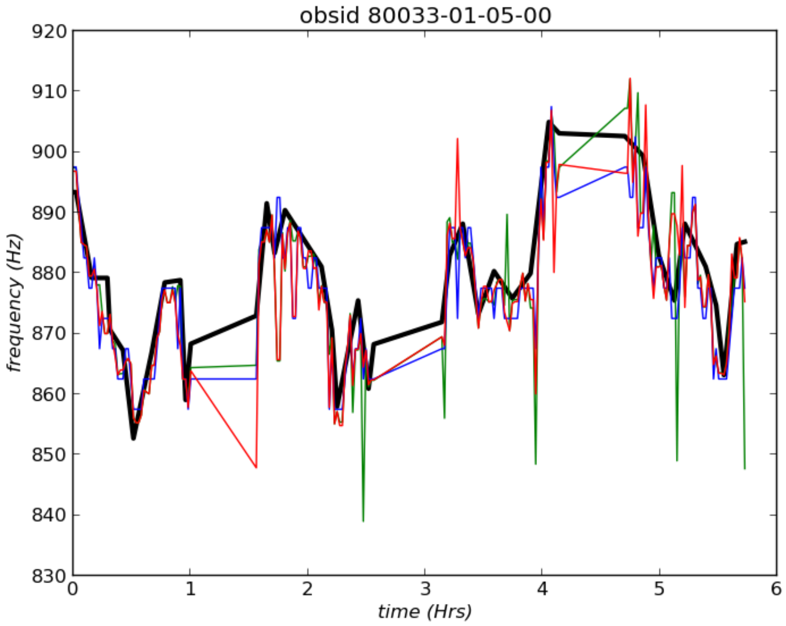

Figure 6: *Time evolution of the lower QPO frequency in observation 80033-01-05-00 of X-ray source 4U 1702–429. The thick black line shows the movement of the QPO frequency as traced by hand, the green line shows the QPO as traced by fitting Lorentzians to each of the power spectra within 50 Hz from the hand selected line. The red line traces the maxima on the individual power spectra within 20 Hz from the peaks of the fitted Lorentzians, and the blue line traces the maxima on the power spectra within 20 Hz from the hand selected line.*

four. 33 gaps, in total, were found. With a short script I found that there are 3176 accepted time intervals, along each of which a centroid frequency and $\dot{\nu}_{QPO}$ can be calculated. These intervals range from 32 s to 176 s. Roughly half of them (1633) fall below 48.0 s, and the other half (1543) are longer.

I wrote a script called *deriv*, that calculates the step derivative and average frequency between every successive pair of data points from all 27 observations, but omits the 33 pairs separated by long gaps, and stores the $\dot{\nu}_{QPO}$ – centroid frequency pairs in a file. It labels every pair as measured on either long or short time intervals by appending a 'q' (for "quick") to every data point measured on an interval shorter than 48 seconds, and appending an 's' (for "slow") to points measured on longer intervals.

Figure 7 shows the $\dot{\nu}_{QPO}$ vs. centroid QPO frequency for every measured interval in every observation. Points with negative $\dot{\nu}_{QPO}$ denote a decrease in QPO frequency. The green plusses are data points measured on time intervals below 48 s, the blue ones are data points measured on longer time intervals.

As can clearly be seen in figure 7, there are many points which share nearly the same $\dot{\nu}_{QPO}$ value for different centroid frequencies. This is of course not a physical phenomenon, but rather the effect of losses in frequency resolution due to rebinning. After rebinning in frequency, the frequency resolution becomes in the order of four Hertz, depending on the actual frequency rebin factor. All points within one bin of this resolution will be shown at the average frequency of that bin.

My script, *databinner* divided – taking "slow" and "quick" data separately - the data in 17 bins with a width of 20 Hz, and calculated the spread of the $\dot{\nu}_{QPO}$ distribution within each bin.

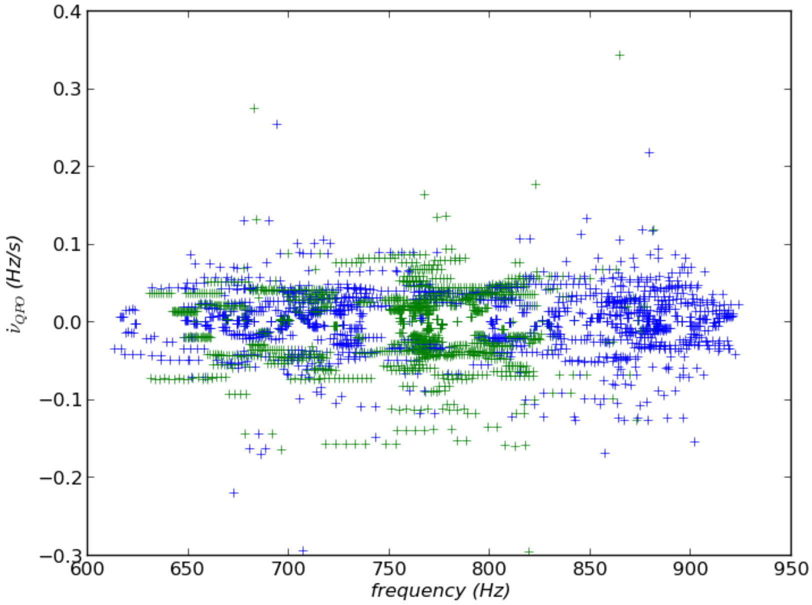

Figure 7: *$\dot{\nu}_{QPO}$ versus centroid frequency of the QPO found in neutron star 4U 1702–429. The green plusses are data measured on time intervals below 48 seconds, the blue plusses are data measured on time intervals above 48 seconds.*

For both slow and quick data, the negative and positive movements in figure 7 seem to mirror each other to an appreciable degree. If this means that there is a coupling between the physical mechanisms which increase and decrease the QPO frequency, we can combine the data, and plot the absolute value of the time-derivative of the QPO freuqency ($|\dot{\nu}_{QPO}|$), and thus decrease the spread of the distribution. Figure 8 shows for every centroid frequency bin the average $|\dot{\nu}_{QPO}|$, the error bars show the distribution of the data points. Blue data is slow, and green data is quick. Note that the error bars do not show actual statistical errors of the data, since errors in measurement and calculation of the derivatives are not taken into account. As figure 8 shows, the behaviour of quick and slow data are very similar. This entitled me to take also these two types of data together and further decrease the $\dot{\nu}_{QPO}$ spreads of the bins. The result is shown in figure 9, the increase of $|\dot{\nu}_{QPO}|$ in the lower half of the frequency range as well as its decrease in the upper half are more pronounced here, but still not very significant as the highest average in the middle hardly exceeds the upper errors at the ends of the frequency range.

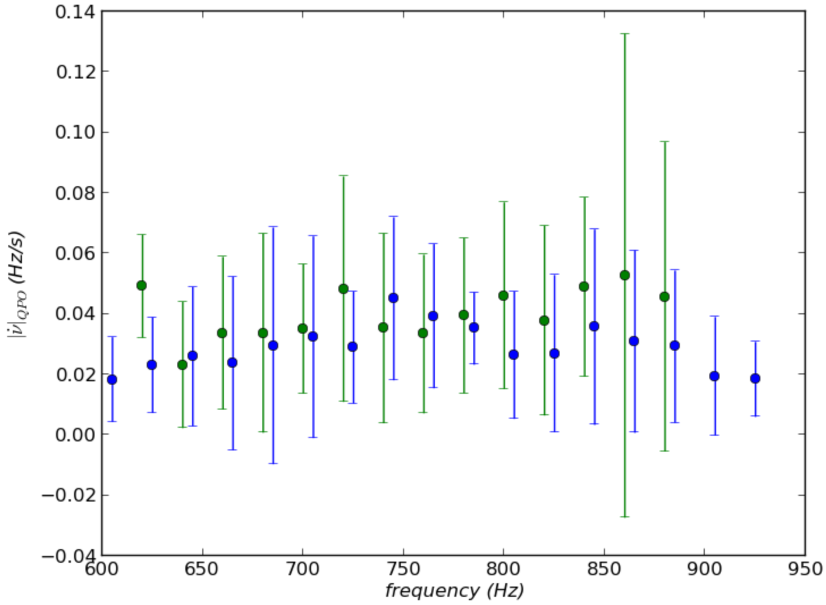

Figure 8: $|\dot{\nu}_{QPO}|$ *plotted against the QPO centroid frequency itself. Green data show derivatives measured over time intervals shorter than 48 seconds, blue data show derivatives measured over longer time intervals. The data is grouped in 17 bins of 20 Hz each. The quick and slow data are shown some space apart, for visual clarity, but belong to the same bin.*

3 Results

The frequency separation between upper and lower QPOs in neutron star 4U 1702 is 340 ± 14.0 Hz, measured over 6 observations with upper QPO significance close to 3σ. The hard colours of the 4U 1702 spectra are relatively high. Reasons for this could be large interstellar absorption, and dominance of the radiation component of the corona over that of the neutron star surface.

1633 pairs of data ($\dot{\nu}_{QPO}$ and centroid QPO frequency) were calculated on time intervals shorter than 48 seconds. 1543 pairs of data on longer intervals. Slow data roughly range from 600 to 940 Hz, quick data range from 620 to 880 Hz.

Positive and negative $\dot{\nu}_{QPO}$ values have similar magnitudes at every measured frequency. This also holds if we take quick and slow data separately. If the QPO frequency is a measure of the orbital radius of a body of matter in the accretion disc, this means that the mechanisms which are responsible for inward and outward movement of this orbit are probably coupled. This is in agreement with findings of Sanna et al. (2012) concearning neutron star 4U 1636–53.

There is no significant correlation or anticorrelation between $\dot{\nu}_{QPO}$ and centroid QPO frequency. There is at best a very mild increase of the derivative with frequencies from 600 to 775 Hz, and a mild decrease at frequencies from there up to 925 Hz, but the $|\dot{\nu}_{QPO}|$ behaviour can best be described as staying anywhere below a roughly constant upper boundary of 0.065 Hz s^{-1}. This result does not contradict the findings of Sanna et al. 2012, who found a clear anticorrelation between $|\dot{\nu}_{QPO}|$ and the centroid QPO frequency of neutron star 4U 1636–53. Their $|\dot{\nu}_{QPO}|$ values remained below the upper boundary I measured at all frequencies.

Within the errors in my data, the trend of $|\dot{\nu}_{QPO}|$ against centroid QPO frequency is invariant between the two ranges of time intervals over which the $|\dot{\nu}_{QPO}|$ values were calculated. This, too, does neither contradict nor reaffirm the findings by Sanna et al. (2012), who found

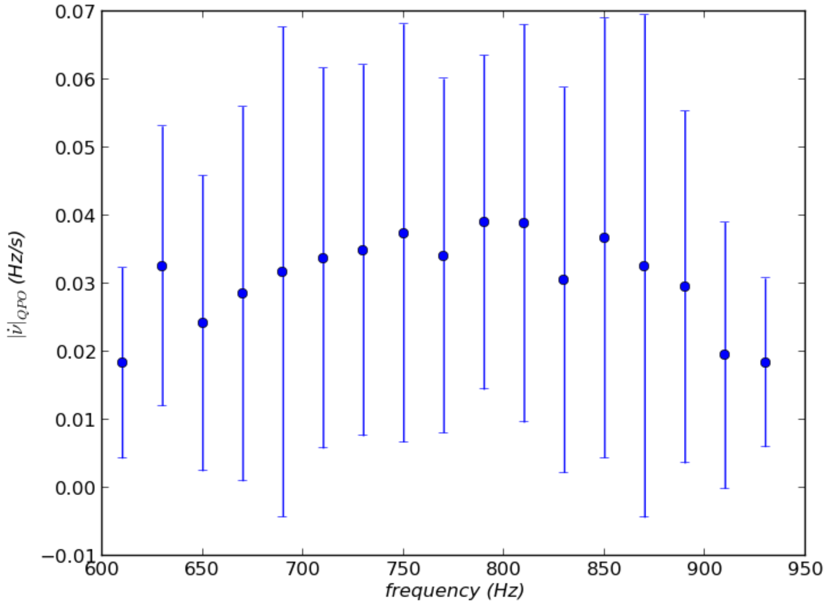

Figure 9: $|\dot{\nu}_{QPO}|$ *from X_ray source 4U 1702–429 plotted against the QPO centroid frequency itself. Both quick (derivatives calculated over time intervals below 48 s) and slow (those calculated over time intervals exceeding 48 s) data are taken together.*

a factor 2 decrease of $|\dot{\nu}_{QPO}|$ as the time interval increases from less than 64 s to 160 s.

From the six observations which show two QPOs simultaneously, I plotted both upper and lower QPO frequencies together, and to appreciable accuracy found a linear relation between 640 and 750 Hz. Fitting a linear regression to these six data points, the relation seems to be:

$$\nu_{upper} = 1.04\nu_{lower} + 304.3\text{Hz}. \tag{2}$$

(Errors in the slope: ± 0.26 ; errors in the intercept: ± 7.9) Belloni et al. (2005) also found a linear relation between the upper and lower QPO frequencies in neutron star 4U 1636–53: $\nu_{upper} = 0.673\nu_{lower} + 539$ Hz. See figure 10. This linear relation between upper and lower QPO frequencies for neutron star 4U 1702 does not seem to be at variance with the earlier result that the frequency separation between upper and lower QPO frequencies is 340 ± 14.0 Hz.

As can be seen from figure 10, the linear relation between the two QPO frequencies that I fitted does not exclude the relation fitted by Belloni et al. (2005). Even assuming zero errors in their fit, my regression is similar to within 1σ for lower QPO frequencies up to roughly 670 Hz, and within 2σ from that frequency onward.

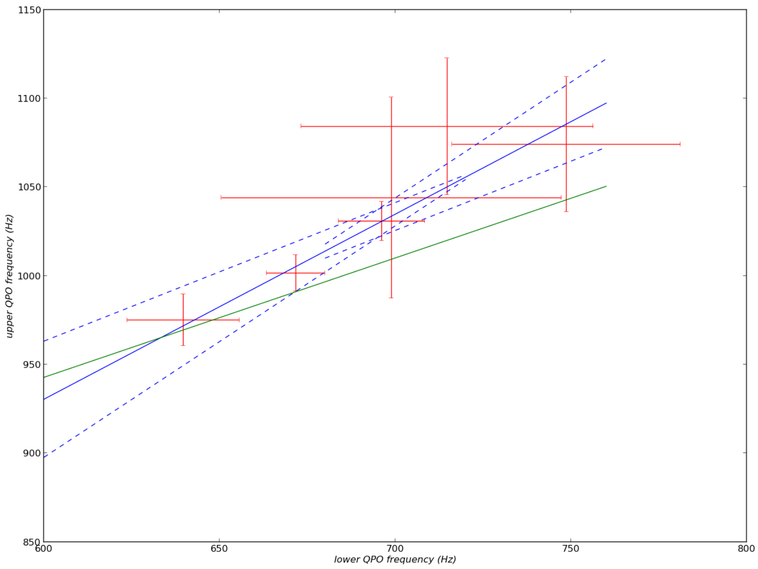

Figure 10: *Six upper QPO frequencies from X-ray source 4U 1702–429 plotted against the frequencies of their respective lower QPOs. The lower QPO errors (in red) were calculated from time-averaged deviations of the lower QPO frequencies from their mean, upper QPO errors were calculated from Lorentzian fit in the Fourier transform. The blue solid line shows the least squares linear fit to this data, the dashed blue lines show the relations with the maximum* $\chi^2 = 1$ *errors in slope and intercept. The solid green line shows the linear fit by Belloni et al. (2005) to the data of neutron star 4U 1636–53.*

4 Discussion and conclusions

4.1 Summary of the results

A linear relation between upper and lower QPO frequencies, as calculated from six measurements with two QPOs is given by: $\nu_{upper} = 1.04\nu_{lower} + 304.3$ Hz. This is appreciably similar to the linear fit by Belloni et al. (2005) to upper and lower QPO frequencies in X-ray source U4 1636–53. The apparent hard colours of X-ray source 4U 1702 are higher than those of X-ray source 4U 1636–53.

Both positive and negative $\dot{\nu}_{QPO}$ have similar magnitudes at each centroid frequency, this suggests a coupling in the increasing and decreasing mechanisms of the QPO frequency. $|\dot{\nu}_{QPO}|$ values have been calculated on time intervals between 32 and 48 s, and occurred at frequencies between 620 and 88 Hz. Those calculated on time intervals between 48 and 176 s occurred at frequencies between 600 and 940 Hz. The absolute data remain under an upper boundary of 0.065 Hz s^{-1} across the entire centroid frequency range. This is not in contrast to the findings by Sanna et al. (2012), but with far less QPO observations, the spreads in my data are too large to verify them.

4.2 Comparison with models

In order to compare his findings to the models of disc theory, Andrea Sanna wrote a *Matlab* routine that simulates the time-evolution of a QPO frequency, assuming the QPO frequency to be the orbital frequency of a body of matter in the accretion disc. An increase in QPO frequency then corresponds to a decrease in the radius of the body's orbit.

Combining the standard disc theory by Shakura & Sunyaev (1973) with the assumption of Keplerian orbit, the absolute derivative of QPO frequency can be expressed as a function of mass accretion rate, neutron star mass, neutron star radius and other quantities. Sanna et al. (2012) have found a theory limited to Shakura & Sunyaev disc theory with an unspecified truncation mechanism to be at variance with the data from neutron star 4U 1636–53. If the sonic-point radius is taken to be the radius of disc truncation, and radiation from accreting matter is assumed to remove angular momentum from the disc by means of radiation drag, Miller et al. (1998) give the approximate sonic-point radius as a function of the neutron star radius, mass accretion rate, the relative thickness of the disc and the radial velocity of the gas in the disc:

$$R_{sr} = R + 5\left(\frac{\dot{M}_i}{0.01\dot{M}_E}\right)^{-1}\left(\frac{R}{10\text{km}}\right)\left(\frac{h/r}{0.1}\right)\left(\frac{v^r}{10^{-5}\text{c}}\right) \tag{3}$$

(Sanna et al. 2012). Assuming a (near) Keplerian orbit again, the absolute value of the time-derivative of the QPO frequency as a function of neutron star mass and the change in sonic-point radius is given by:

$$|\dot{\nu}_{sr}| = \frac{3}{4\pi}(GM)^{1/2}R_{sr}^{-5/2}|\dot{R}_{sr}| \tag{4}$$

with

$$|\dot{R}_{sr}| \approx 0.05\dot{M}_E\left(\frac{\dot{M}_i}{0.01\dot{M}_E}\right)^{-2}\ddot{M}_i\left(\frac{R}{10\text{km}}\right)\left(\frac{h/r}{0.1}\right)\left(\frac{v^r}{10^{-5}\text{c}}\right) \tag{5}$$

where R is the neutron star radius in km, $\dot{M}_i$ is the mass accretion rate through the disc, $\dot{M}_E$ is the Eddington mass accretion rate, h is the thickness of the disc at a radial distance r, v^r is the radial velocity of the gas in the accretion disc, and $\ddot{M}_i$ is the time-derivative of the mass accretion rate through the disc. (Sanna et al. 2012). The Eddington mass accretion rate $\dot{M}_E$ is the mass accretion rate which corresponds to the Eddington luminosity L_E following the relation $L_E = GM\dot{M}_E/R_\star$. Here, the Eddington luminosity L_E is the luminosity of a body at which the outward radiation pressure precisely counteracts the gravitational attraction of surrounding matter. (Frank, King and Raine, 1985).

Andrea Sanna's routine uses these equations in combination with random numbers to simulate a possible course of QPO frequency for given values of maximum and minimum mass accretion rate, neutron star mass, neutron star radius and time interval over which the $\dot{\nu}_{QPO}$ values are calculated. It presumes the relative thickness of the disc (thickness over radius) to be 0.1, and the radial velocity of the gas to be 10^{-5}c.

Setting 0.01 and 0.018 times the Eddington mass accretion rate as lower and upper boundaries on the mass accretion rate, and a time step of 90 seconds over which the $\dot{\nu}_{QPO}$ values are calculated, I found the simulated QPO frequency evolution to reflect reasonably well the data of 4U 1702, if the neutron star in the simulation has a radius of 14 km and a mass of 2.5 solar masses. This does not mean that neutron star 4U 1702 has these values for radius and mass, as different values for mass accretion rates, time step, radius and mass may equally well reflect the measured data. What we can conclude from this agreement is that the disc theory plus radiation drag and truncation at the sonic point radius, as it did for neutron star 4U 1636–53, may be a reasonable model for the physics of neutron star 4U 1702. A radius of 14 km is a very normal size for a neutron star. A mass of 2.5 $M_\odot$ is a bit high, the only real concern is that the mass accretion rates in our simulation are rather low compared to what would be expected from theory. The mass accretion rate for a system in which mass accretion is the dominant source of radiation is proportional to the bolometric luminosity of that system (Juhan Frank, Andrew King and Derek Raine - Accretion Power in Astrophysics, 1985). In this case the bolometric luminosity equals the X-ray luminosity to within an error of 50 % (Ford, van der Klis, Mendez et al. 2000). The expected mass accretion rate would then be closer to 0.03 times the Eddington mass accretion rate. This same concern was voiced by Sanna et al. (2012), over the mass accretion rate in their simulation of neutron star 4U 1636–53 being a factor 3 less than the range of luminosities spanned by 4U 1636–53. They note, however, that an adjustment to the relative thickness of the disc and to the radial velocity of the gas may reconcile this problem.

Figure 11 shows the $|\dot{\nu}_{QPO}|$ of neutron star 4U 1702 as measured from the actual observations (red) and as simulated in *matlab* with the parameters as mentioned above (green). The simulated dependence of $|\dot{\nu}_{QPO}|$ on the centroid frequency does not follow the upward curve that is suggested in the measured data, and this would be the most pressing argument against the proposed model.

This comparison between the $\dot{\nu}_{lowerQPO}$ and sonic-point radius orbital frequencies hypothe-

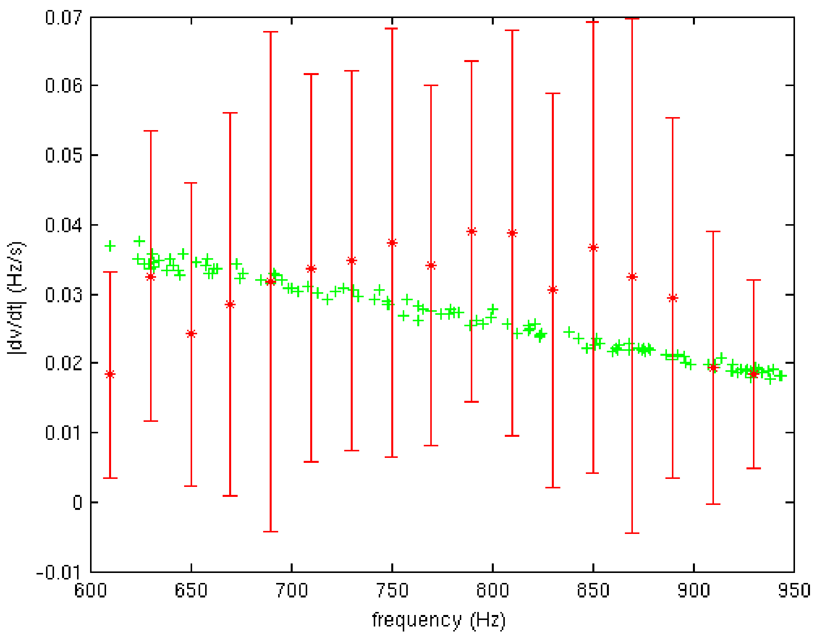

Figure 11: *Red data show the measured $|\dot{\nu}_{QPO}|$, note that the error bars signify the spread in the measurements, not the actual errors. The green data show the absolute time-derivatives of the orbital frequency at the sonic-point radius in the accretion disc, as simulated with a random walk by Andrea Sanna's* matlab *script.*

sises that the lower QPO frequencies are the ones that are Keplerian. Most models, though, assume the upper QPO frequencies to be Keplerian. Using the found linear relation between lower and upper QPO frequencies, I calculated 27 probable upper QPO frequency bins and ran them through Andrea Sanna's routine. Basic algebra dictates that the $|\dot{\nu}_{QPO}|$ values need only be multiplied by the slope of the linear regression in order to get the derivatives of the upper QPOs frequencies.

Figure 12 shows the *matlab* simulation of the sonic-point radius orbital frequency time-derivative, tweaked to approximate the calculated $|\dot{\nu}_{upperQPO}|$. The maximum mass accretion rate is lowered to 0.017 times the Eddington mass accretion rate, the neutron star mass is lowered to 2.4 solar masses (which comes marginally closer to the average neutron star mass), and its radius is lowered to 12 km. Again, these are no mass accretion rate, mass and radius determinations under the assumption that the upper QPO frequency is the Keplerian one. Rather, this shows that the standard disc theory plus radiation drag may model just as well the physics of neutron star 4U 1702 under the assumption that the upper QPO frequency is Keplerian.

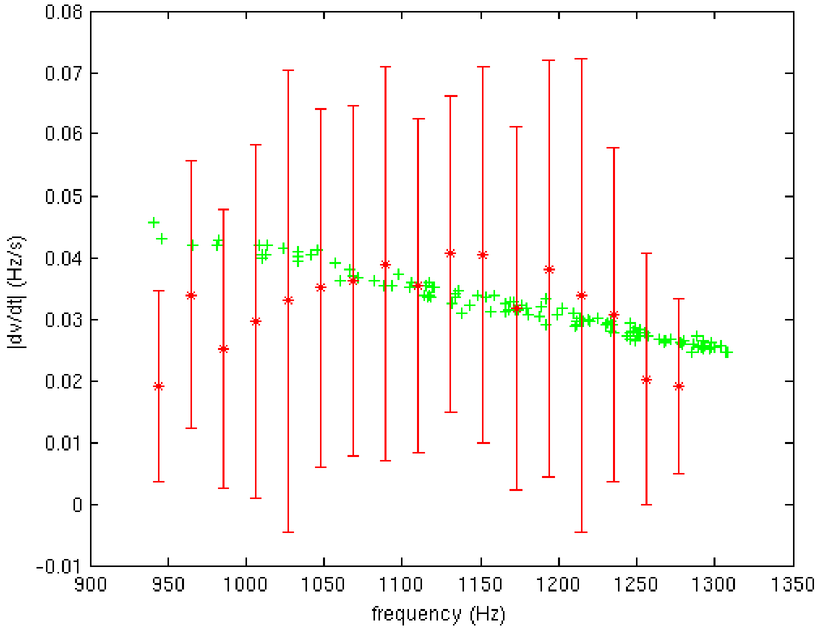

Figure 12: *The red data show the frequency bins (and spreads in the data) of the realistic* $|\dot{\nu}_{upperQPO}|$ *values in neutron star 4U 1702, as calculated from the lower QPO data from the same source. The green data show the time-derivatives of the orbital frequencies at the sonic-point radii as simulated by Andrea Sanna's random walk routine, assuming the following parameters: A relative thickness of the disk (h/r) of 0.1, a radial gas velocity of* $10^{-5}c$*, a lower mass accretion limit of 0.01* $\dot{M}_E$*, an upper mass accretion limit of 0.017* $\dot{M}_E$*, a neutron star mass of 2.4* $M_\odot$ *and a neutron star radius of 12 km.*

4.3 Discussion and summary

Below, I will discuss the caveats in reasoning and limitations of my research.

The moment at which photons from neutron star 4U 1702 are detected with the PCUs, the first errors are a fact. The energy resolution of the PCA is less than 18% at 6 KeV, and there are limitations to the accuracy and consistency with which energies are mapped onto different channels. My research, however, is not concerned with energy variability. I took the Fourier transform of the measurements in the entire energy range, so any error the PCA made in measuring or processing the energy of a photon had not the slightest relevance for my analysis. Only in determining the colours of my spectra did these uncertainties play a role. The program used for calculating these colours took this into account, and the errors in the soft colours were of order 0.008, those in the hard colours of order 0.6. The identification of QPOs was very confident, based also on other methods and the agreement between them. The temporal resolution of the PCA is 1/4096 s ($\approx 244\mu$s), while the accuracy with which the time of an incoming photon is measured is 1 μs. The collecting area of the PCA is sufficient to see time variability in the X-ray signal on the KHz scale with this resolution.

Perhaps the greatest limitation in this research is lack of QPO observations, no more than 27 observations were found that actually show a QPO. A larger amount of data would have decreased the spread in $\dot{\nu}_{QPO}$ calculations, and quite possibly have verified the anticorrelation between $|\dot{\nu}_{QPO}|$ and centroid frequency which has earlier been observed in the neutron star 4U 1636–53 (Sanna et al. 2012).

Dividing the light curves in pieces of 16 s limits the spectral range to a maximum of 2048 Hz, (but QPOs at such high frequencies are definitely not expected). If all resulting transformations are combined, the noise is reduced by a factor equal to the square root of the number of trafos in each observation. In order to make the QPO frequencies and their time-evolutions visible, it was necessary to rebin the power spectra (which had a time resolution of 16 s and a frequency resolution of 1/16 Hz) in time with factors between 1 and 10, and in frequency with factors between 30 and 120. It is conceivable that variations in the QPO frequencies at small timescales which would have pointed to a considerably different $\dot{\nu}_{QPO}$- centroid frequency graph were lost due to this rebinning. This effect would in all expectation affect the $\dot{\nu}_{QPO}$ calculations over shorter time intervals more than those over longer ones. This may well be one reason (besides lack of QPO observations) why my results fail to reflect those of Sanna et al. (2012), who fitted sequences of 4-th degree polynomials on their frequency-time tracks. It has to be noted, though, that the shortest time steps in my research were 32 s, just as long as the shortest ones in the study by Sanna et al. (2012).

Given the two used methods of QPO identification, it is very certain that no upper and lower QPOs were mixed up. Upper and lower QPOs form such distinct groups on the centroid frequency - hard colour plot of the source that misidentification of one QPO is only realistic if all QPOs of that same type are misidentified. This is in itself nearly impossible, as six upper QPOs have been seen alongside their lower frequency twins in the same observation, each with a significance close to 3σ and situated close to the frequencies where an upper QPO would be expected. The 3σ significant upper QPOs were found by fitting Lorentzians (plus constants of order 2) to the average of the separate trafos of each observation where they were taken together in such a way that the lower QPO frequencies of all separate trafos would coincide. The errors on the measured upper QPO frequencies were calculated from the frequency ranges over which different trafos were shifted, assuming a uniform distribution in trafo shift frequencies for each observation.

In the six observations which show two QPOs, the errors on the upper and lower QPO frequencies vary between 8.3 and 57 Hz. Nonetheless, they appear to quite closely follow a linear relation on the upper frequency - lower frequency plane. The slope of the linear fit is 1.04 ± 0.26 and the intercept value is 304.3 ± 7.9 Hz. The errors in the fit were calculated from those in the fitted data.

Determining the time-evolution of the lower QPO frequencies was done manually by selecting a sequence of points in the frequency-time plane of each observation. Despite considerable rebinning, the noise in the Fourier powers in these sequences of transformations was so high that automatic selection of maxima, fitting of Lorentzians to the frequency profiles, or combinations of these methods yielded far too much unphysical fluctuation in the time-evolution of the QPO frequencies, manual selection was the only feasible way to avoid this.

The identification of 33 unacceptably long time intervals over which the calculation of $\dot{\nu}_{QPO}$ values would not yield physical data was done with considerable certainty. Each time interval considered was either obviously acceptable (i.e. hardly any longer than the usual time interval in that observation) or obviously too long (i.e. a lot more than twice the usual time interval).

When separate points on the $\dot{\nu}_{QPO}$-centroid frequency plots were grouped into several frequency bins, the frequency bins were plotted with error bars indicating nothing more than the spreads of the data points in each bin. Errors which accumulated during measurement, Fourier transformation, rebinning, and QPO frequency-time tracing were not taken into account. Most of the errors were presumably built up with rebinning and with the manual tracing of the time-evolution of the lower QPO frequencies. Information on the magnitude of these errors is not easily estimated.

Combining two groups of data (i.e. positive and negative $\dot{\nu}_{QPO}$ values) decreases the spreads in the bins, but division of these bins into two different groups (i.e. 'quick' and 'slow' data) counteracts this effect. The final behaviour of quick and slow data in the $\dot{\nu}_{QPO}$-centroid frequency plot are so similar, though, that they could be taken together, and a more accurate (i.e. less spreaded) frequency evolution of $|\dot{\nu}_{QPO}|$ was found. It cannot be ruled out that the resulting plot shows a physical increase and decrease in $\dot{\nu}_{QPO}$ over the measured frequency range.

The found $|\dot{\nu}_{lowerQPO}|$ values, plotted against the centroid frequencies of these lower QPOs can be reproduced in a random walk simulation, given reasonable parameters for the simulated neutron star, (thickness over radius = 0.1, radial velocity of the gas in the disc = 10^{-5}c, minimum mass accretion rate = 0.01 $\dot{M}_E$, maximum mass accretion rate = 0.018 $\dot{M}_E$, neutron star radius = 14 km, neutron star mass = 2.5 $M_\odot$). This simulated neutron star is certainly heavier than usual, but especially given the possible errors in the $\dot{\nu}_{QPO}$ values, the tested model of standard disc theory with radiation drag, assuming the lower QPO frequency to be the frequency of the sonic-point radius in the disc can not be ruled out.

Assuming (as most proposed theories do) that the upper QPO frequency is the one corresponding to an orbit at the sonic-point radius in the disc, the model can be fitted to a collection of probable $|\dot{\nu}_{upperQPO}|$ versus their centroid frequencies. This upper QPO frequency data can be calculated from the measured lower frequency QPO data with the fitted linear regression between upper and lower QPO frequencies. In this process, the errors in the linear fit also propagate into the final comparison with the model. The upper QPO data can be reproduced with the same model if the upper mass accretion rate is lowered to 0.017 $\dot{M}_E$, the mass is lowered to 2.4 $M_\odot$ and the radius is lowered to 12 km. Provided that the unusually low mass accretion rate can be accounted for by the assumption of relative thickness to be 0.1, these values come marginally closer to the average for neutron stars. This hardly makes the model with the upper QPO frequency as sonic-point frequency better than the one with the lower QPO frequency fulfilling that role, since the errors in the calculated upper QPO data are larger.

5 Epilogue

In my research of neutron star 4U 1702–429, I found among other things a relation between upper and lower QPO frequencies, separate branching of the upper and lower QPOs on the frequency-hard colour plane, likely coupling of mechanisms for increase and decrease of QPO frequency, a possibility (within the errors in my data) of anticorrelation between $|\dot{\nu}_{QPO}|$ and centroid frequency, and a reasonable consistency between measured data and data reproduced by the model of standard disc theory, sonic-point radius and radiation drag. These five findings are in agreement with earlier results from studies of the neutron star 4U 1636–53 (Belloni et al. 2005; Sanna et al. 2012). These agreements point towards a universal occurrence of the mentioned properties in many and perhaps all neutron star accretion discs, and perhaps other X-ray bright objects. This should be verified by studying the time evolution of QPO frequencies in other neutron stars.

6 Acknowledgements and references

With thanks to Mariano Méndez, for his guidance during my research in its entirety, for providing valuable insights in the topic, and constructive comments on the manuscript. Thanks to Andrea Sanna for providing me with the RXTE data to start with, for lending his implementation of the disc theory models, and for his experienced advice. Thanks to Guobao Zhang, for helping with the QPO identification.

Articles:

· Hasinger, G.; van der Klis, M. Astronomy and Astrophysics (ISSN 0004-6361), vol. 225, no. 1, Nov. 1989, p. 79-96.

· Altamirano, D.; van der Klis, M.; Méndez, M.; Wijnands, R.; Markwardt, C.; Swank, J. The Astrophysical Journal, Volume 687, Issue 1, pp. 488-504.

· Altamirano, D.; Wijnands, R.; van der Klis, M.; Mendez, M. 36th COSPAR Scientific Assembly. Held 16 - 23 July 2006, in Beijing, China. Meeting abstract from the CDROM, #1391

· Barret, D.; Olive, J.-F.; Miller, M. Coleman Astronomische Nachrichten, Vol.326, Issue 9, p.808-811

· Belloni, T.; Homan, J.; Motta, S.; Ratti, E.; Méndez, M. Monthly Notices of the Royal Astronomical Society, Volume 379, Issue 1, pp. 247-252.

· Belloni, T.; Méndez, M.; Homan, J. Astronomy and Astrophysics, Volume 437, Issue 1, July I 2005, pp.209-216

· Berger, M.; van der Klis, M.; van Paradijs, J.; Lewin, W. H. G.; Lamb, F.; Vaughan, B.; Kuulkers, E.; Augusteijn, T.; Zhang, W.; Marshall, F. E.; Swank, J. H.; Lapidus, I.; Lochner, J. C.; Strohmayer, T. E. Astrophysical Journal Letters v.469, p.L13

· Di Salvo, T.; Méndez, M.; van der Klis, M.; Ford, E.; Robba, N. R. The Astrophysical Journal, Volume 546, Issue 2, pp. 1107-1120.

· Ford, Eric C.; van der Klis, Michiel; Méndez, Mariano; Wijnands, Rudy; Homan, Jeroen; Jonker, Peter G.; van Paradijs, Jan The Astrophysical Journal, Volume 537, Issue 1, pp. 368-373.

· Markwardt, Craig B.; Strohmayer, Tod E.; Swank, Jean H. The Astrophysical Journal, Volume 512, Issue 2, pp. L125-L129.

· Méndez, M.; van der Klis, M.; Ford, E. C.; Wijnands, R.; van Paradijs, J. The Astrophysical Journal, Volume 511, Issue 1, pp. L49-L52.

· Méndez, Mariano; van der Klis, Michiel The Astrophysical Journal, Volume 517, Issue 1, pp. L51-L54.

· Miller, M. Coleman; Lamb, Frederick K.; Psaltis, Dimitrios The Astrophysical Journal, Volume 508, Issue 2, pp. 791-830.

· Sanna, Andrea; Méndez, Mariano; Belloni, Tomaso; Altamirano, Diego Monthly Notices of the Royal Astronomical Society, Volume 424, Issue 4, pp. 2936-2942.

· Shakura, N. I.; Sunyaev, R. A. Astronomy and Astrophysics, Vol. 24, p. 337 - 355

· Stella, Luigi; Vietri, Mario Astrophysical Journal Letters v.492, p.L59

· Strohmayer, T.; Zhang, W.; Swank, J. IAU Circ., 6320, 1 (1996). Edited by Green, D. W. E.

· van der Klis, M. Astronomische Nachrichten, Vol.326, Issue 9, p.798-803

Books:

· Bendat, Piersol 'Random Data, Analysis and Measurement Procedures', 2010

· Juhan Frank, Andrew King and Derek Raine 'Accretion Power in Astrophysics', 1985.